Supplementary Information

A Series of Anionic MOFs with Cluster-Based, Pillared-Layer and Rod-Spacer Motifs: Near-Sunlight White-Light Emission and Selective Dye Capture

Ce Wang,[a] Zheng Yin,*[a] Zhao Cheng,[b] Wei-Min Ma,[a] Xi-Yao Li,[a] Xiao-Ting Hu,[c] Rong Shi,[a] Ao-Wei Chen[a] and Yang-Min Ma.*[a]

[a] College of Chemistry and Chemical Engineering, Shaanxi Key Laboratory of Chemical Additives for Industry, Shaanxi University of Science and Technology, Xi'an 710021, P. R. China.

[b] School of Pharmaceutical, Xi'an Medical University, Xi'an, 710021, P. R. China.

[c] College of Chemistry and Chemical Engineering, Hubei University, Wuhan, 430062, P. R. China.

Table S1 Statistical of typical anionic and neutral MOFs with d^{10} metal, and COFs based compounds with white-light emission in the literatures.

Types	Compounds	Structure Features	Fluorescent Properties	Ref.
Anionic MOFs	$[Me_2NH_2]_6[Zn_{16}(btc)_{12}(gac)(DMA)_3(H_2O)_3]\cdot$guest H_3btc = benzene-1,3,5-tricarboxylic acid	Pillared-layer framework with sophisticated crystallographic asymmetric unit	Continuous broadband white-light emission with CIE coordinates of (0.298, 0.333) under excitation of 360 nm	[1]
	$[Zn_2(L)\cdot H_2O]\cdot 3H_2O\cdot 3DMAc\cdot NH_2(CH_3)_2\}_n$ H_5L = 3,5-bis(1-methoxy-3,5-benzene dicarboxylic acid)benzoic acid	5-connected *vbk* net containing 1D nanotubular channels	The MOFs with $0.183Eu^{3+}$ and $0.408Tb^{3+}$ exhibited white emission with CIE coordinates of (0.339, 0.327) and Φ_{PL} of 8%, under excitation of 359 nm	[2]
	$[(CH_3)_2NH_2]_{15}[(Cd_2Cl)_3(TATPT)_4]\cdot 12DMF\cdot 18H_2O$ H_6TATPT = 2,4,6-tris(2,5-dicarboxylphenylamino)-1,3,5-triazine	3D mesoporous MOFs containing 2 and 3 nm cages	MOFs with 3.5 wt% $[Ir(ppy)_2(bpy)]^+$ exhibited white emission with CIE coordinates of (0.31, 0.33) and high Φ_{PL} of 20.4% under excitation of 370 nm	[3]
	$(Me_2NH_2)[Zn_2(L)(H_2O)]\cdot 4DMA$ H_5L = 2,5-(6-(3-carboxy phenylamino)-1,3,5-triazine-2,4-diyl-diimino	A 3D anionic *bcu-f* network	Iridium and ruthenium complex encapsulated MOFs exhibited white emission with CIE coordinates of (0.33, 0.34)	[4]
	$[Me_2NH_2][Cd(btc)]\cdot 0.5DMA\cdot 2H_2O$	(3, 6) connected α-PbO_2 framework	Dual emission at 390 nm and 515 nm with CIE coordinate of (0.317, 0.365) and Φ_{PL} of 5.17%, under excitation of 350 nm	This work
Neutral MOFs	$[Cd(tzphtpy)_2]\cdot 6.5H_2O$ Htzphtpy = 4-(tetrazol-5-yl)phenyl-2,2′:6′,2″-terpyridine	1D chain with intra-/intermolecular π–π interactions	Dual emission with CIE coordinate of (0.33, 0.36) and Φ_{PL} of 2.3% under excitation of 326 nm	[5]
	$[Cd_5(HTTHA)_2(Hpt)_4(H_2O)]\cdot 4H_2O$ H_6TTHA = 1,3,5-triazine-2,4,6-triamine hexaacetic acid, Hpt = pyridinium-4-thiolate	2D network	Broad emission covering the entire visible spectrum with CIE coordinate of (0.34, 0.36) and Φ_{PL} of 16.02% under 10 K and excitation of 360 nm	[6]
	$[Zn(mim)_2]$ (ZIF-8) Hmim= 2-methylimidazole	3D SOD topology framework	Continuous broadband white-light emission with CIE coordinates of (0.290, 0.339) and Φ_{PL} of 4.73%, under excitation of 365 nm	[7]
	$Zn(L)(Hbtc)(H_2O)_2$ L = N,N'-di(pyridin-4-yl)biphenyl-4,4'-dicarboxamide	3D framework with 1D regular hexagonal channels	Dual emission peaks at 424 and 539 nm with comparable intensity, resulting in direct white-light emission, under excitation of 373 nm	[8]
	$\{[Zn_6(HPI)_4(HPI2C)_4]\cdot (DMF)_5(H_2O)_3\}_n$	(1D) ribbon-like chain	Dual emission peaks at 408 and 555 nm with CIE coordinates of (0.28, 0.28)	[9]

COFs	IISERP-COF7	Anthracene-resorcinol based 2D COF with uniform 1-D channels	A 0.32 wt% loading of the COF in PMMA gives a solvent-free film with intense white emission with CIE of (0.35,0.36)	[10]
	Tf-DHzDAll	Eclipse-stacked 2D COFs with intralayer and interlayer hydrogen bonds	Dual emission having CIE of (0.31, 0.4) under 365 nm excitation with Φ_{PL} of 11.9%	[11]
	Eu^{3+}/Tb^{3+} grafted TTA-DFP-COF	2D imine COF with nitrogen-rich pockets to anchor lanthanides	10%Eu,90%Tb@TTA-DFP give emission with CIE of (0.3636, 0.3355) under 340 nm excitation with Φ_{PL} of 3.1%	[12]

Reference:

[1] C. Wang, Z. Yin, W.-M. Ma, X.-Y. Li, L.-H. Cao, Y. Cheng, X.-Y. Yu and Y.-M. Ma, *Dalton Trans.* 2019, **48**, 14966-14970.

[2] M.-L. Ma,; J.-H. Qin, C. Ji, H. Xu, R. Wang, B.-J. Li, S.-Q. Zang, H.-W. Hou and S. R. Batten, *J. Mater. Chem. C* 2014, **2**, 1085-1093.

[3] C.-Y. Sun, X.-L. Wang, X. Zhang, C. Qin, P. Li, Z.-M. Su, D.-X. Zhu, G.-G. Shan, K.-Z. Shao, H. Wu and J. Li, *Nature Commun.* 2013, **4**, 2717.

[4] H. Zhao, J. Ni, J.-J. Zhang, S.-Q. Liu, Y.-J. Sun, H. Zhou, Y.-Q. Li and C.-Y. Duan, *Chem. Sci.* 2018, **9**, 2918-2926.

[5] R. Li, S.-H. Wang, Z.-F. Liu, X.-X. Chen, Y. Xiao, F.-K. Zheng and G.-C. Guo, *Cryst. Growth Des.* 2016, **16**, 3969-3975.

[6] Q. Zhu, T. Sheng, C. Tan, S. Hu, R. Fu and X. Wu, *Inorg. Chem.* 2011, **50**, 7618-7624.

[7] X. Yang and D. Yan, *Chem. Commun.* 2017, **53**, 1801-1804.

[8] F. Luo, M.-S. Wang, M.-B. Luo, G.-M. Sun, Y.-M. Song, P.-X. Li and G.-C. Guo, *Chem. Commun.* 2012, **48**, 5989-5991.

[9] L. Chen, C. Yan, M. Pan, H.-P. Wang, Y.-N. Fan and C.-Y. Su, *Eur. J. Inorg. Chem.* 2016, 2676-2680.

[10] S. Haldar, D. Chakraborty, B. Roy, G. Banappanavar, K. Rinku, D. Mullangi, P. Hazra, D. Kabra and R. Vaidhyanathan, *J. Am. Chem. Soc.* 2018, **140**, 13367-13374.

[11] X. Li, Q. Gao, J. Wang, Y. Chen, Z.-H. Chen, H.-S. Xu, W. Tang, K. Leng, G.-H. Ning, J. Wu, Q.-H. Xu, S. Y. Quek, Y. Lu and K. P. Loh, *Nature Commun.* 2018, **9**, 2335.

[12] C. Krishnaraj, A. M. Kaczmarek, H. S. Jena, K. Leus, N. Chaoui, J. Schmidt, R. Van Deun and P. Van Der Voort, *ACS Appl. Mater. Inter.* 2019, **11**, 27343-27352.

Table S2 Statistical of typical anionic btc-MOFs in the literatures.

No.	Formula	Structure Features	References
1	$(HTEA)_2[Zn_3O(btc)_2]$	(3,6)-connected network	*J. Am. Chem.* Soc. **2001**, *123*, 8239.
2	$[NH_2(CH_3)_2]_2[Zn_3(bdc)_2(btc)_2(NH(CH_3))_2]$	3D framework with 1D channels	*Inorg. Chem.* **2003**, *42*, 944.
3	$[NH_2(CH_3)_2][Cd(btc)]\cdot DMA$	3D framework with the rutile topology containing 1D channels	*Sci. China. Chem*. **2010**, *53*, 2144.
4	$[NH_2(CH_3)_2]_3[(Cu_4Cl)_3(btc)_8]_9\cdot DMA$	(3,8)-connected net with sodalite-type cages	*Chem. Commun.* **2011**, *47*, 10647.
5	$[NH_2(CH_3)_2](H_2bhep)[Zn_3(btc)_3]$	3D framework contains large wheel-shaped and hexagonal cavities	*Cryst. Growth Des.* **2012**, *12*, 5471.
6	$(NMe_4)[Zn(btc)]$	3D framework	*Cryst. Growth Des.* **2014**, *14*, 5452.
7	$(HTEA)_4[Zn_5(btc)_2(Hbtc)_4]$	3D framework with 1D rhombic channels	*Inorg. Chem.* **2014**, *53*, 691.
8	$[NH_2(CH_3)_2][Cd(btc)]\cdot DMA$	binodal (3,6)-connected rutile topology	*Chem. Commun*. **2015**, *51*, 14211.
9	$[NH_2(CH_3)_2]_2[Mn_2Cl_2(btc)_{4/3}]\cdot 4/3H_2O$	(3,4)-connected 3D tbo framework	*Cryst. Growth Des.* **2016**, *16*, 6776.
10	$[NH_2(CH_3)_2]_2[Mn_3(btc)_2(CH_3COO)_2]$	(3,n)-connected network	*New J. Chem.* **2016**, *40*, 2680.

Table S3 Crystal data and refinement details for **1**.

Empirical formula	$CdC_{13}H_{19.5}N_{1.5}O_{8.5}$
Formula weight	445.21
Temperature / K	100
Radiation / Å	1.54184 (Cu *K*α)
Crystal system	Orthorhombic
Space group	*Pbcn*
a / Å	12.5634 (3)
b / Å	16.1618 (3)
c / Å	17.1222 (3)
α / °	90
β / °	90
γ / °	90
V / Å^3	3476.59 (12)
Z	8
F(000)	1440
D_c./ g cm^{-3}	1.397
μ / mm^{-1}	10.24
Reflns coll.	11188
Unique reflns.	3515
R_{int}	0.031
$^aR_1$ [I$\geqslant$2σ(I)]	0.041
$^bWr_2$ (all data)	0.136
GOF	1.12
Void	55.5%
CCDC number	1943117

$^aR_1 = \sum||F_o| - |F_c||/\sum|F_o|$. $^bwR_2 = [\sum w(F_o^2 - F_c^2)^2/\sum w(F_o^2)^2]^{1/2}$.

Table S4 The selected bond lengths and bond angles of **1**.

Bond lengths			
Cd1—O1	2.257 (3)	Cd1—O4^{iii}	2.389 (3)
Cd1—O2^{i}	2.257 (3)	Cd1—O3^{iv}	2.491 (3)
Cd1—O5^{ii}	2.403 (3)	Cd1—O4^{iv}	2.422 (3)
Cd1—O6^{ii}	2.307 (3)		
Bond angles			
O1—Cd1—O5^{ii}	142.26 (9)	O5^{ii}—Cd1—O3^{iv}	79.01 (10)
O1—Cd1—O6^{ii}	88.45 (10)	O5^{ii}—Cd1—O4^{iv}	130.49 (10)
O1—Cd1—C9^{ii}	115.80 (11)	O6^{ii}—Cd1—O5^{ii}	55.75 (10)
O1—Cd1—O4^{iii}	120.37 (10)	O6^{ii}—Cd1—O4^{iii}	149.69 (10)
O1—Cd1—O3^{iv}	116.59 (11)	O6^{ii}—Cd1—O3^{iv}	90.74 (12)
O1—Cd1—O4^{iv}	79.25 (9)	O6^{ii}—Cd1—O4^{iv}	128.04 (11)
O2^{i}—Cd1—O1	85.31 (11)	O2^{i}—Cd1—O4^{iii}	74.69 (11)
O2^{i}—Cd1—O5^{ii}	89.81 (10)	O2^{i}—Cd1—O3^{iv}	155.71 (11)
O2^{i}—Cd1—O6^{ii}	100.74 (12)	O2^{i}—Cd1—O4^{iv}	127.74 (10)

Symmetry codes: (i) -*x*+2, *y*, -*z*+3/2; (ii) -*x*+3/2, -*y*+1/2, *z*+1/2; (iii) *x*+1/2, *y*-1/2, -*z*+3/2; (iv) -*x*+3/2, *y*-1/2, *z*; (v) -*x*+3/2, -*y*+1/2, *z*-1/2; (vi) *x*-1/2, *y*+1/2, -*z*+3/2; (vii) -*x*+3/2, *y*+1/2, *z*.

Table S5 Crystal data and refinement details for **2**.

Empirical formula	$Cd_5C_{41}H_{56}N_5O_{28}$
Formula weight	1628.96
Temperature / K	293
Radiation / Å	0.71073 (Mo *Kα*)
Crystal system	Monoclinic
Space group	$P2_1/c$
a / Å	20.1064 (5)
b / Å	14.0180 (4)
c / Å	18.9293 (5)
α / °	90
β / °	118.072 (2)
γ / °	90
V / Å^3	4707.6 (2)
Z	4
F(000)	2448
D_c./ g cm^{-3}	1.818
μ / mm^{-1}	2.29
Reflns coll.	37310
Unique reflns.	11527
R_{int}	0.056
$^aR_1$ [I$\geqslant$2σ(I)]	0.231
$^bwR_2$ (all data)	0.674
GOF	1.07
Void	29.2%
CCDC number	1943118

$^aR_1 = \sum||F_o| - |F_c||/\sum|F_o|$. $^bwR_2 = [\sum w(F_o^2 - F_c^2)^2/\sum w(F_o^2)^2]^{1/2}$.

Table S6 The selected bond lengths and bond angles of **2**.

Bond lengths			
Cd1—O1	2.462 (13)	Cd3—O16^{iii}	2.109 (9)
Cd1—O2	2.281 (9)	Cd4—O4	2.233 (15)
Cd1—O7	2.229 (16)	Cd4—O24	2.51 (2)
Cd1—O19	2.271 (15)	Cd4—O5^{iv}	2.518 (15)
Cd1—O10^{i}	2.321 (11)	Cd4—O6^{iv}	2.39 (3)
Cd1—O14^{ii}	2.266 (6)	Cd4—O11^{v}	2.327 (11)
Cd2—O8	2.238 (13)	Cd4—O12^{v}	2.440 (8)
Cd2—O13	2.312 (6)	Cd4—O17^{vi}	2.447 (7)
Cd2—O15	2.324 (6)	Cd5—O6	2.26 (3)
Cd2—O20	2.288 (17)	Cd5—O21	2.23 (2)
Cd2—O10^{i}	2.218 (11)	Cd5—O22	2.39 (4)
Cd2—O13^{ii}	2.264 (5)	Cd5—O25	2.31 (2)
Cd3—O6	2.62 (4)	Cd5—O3^{i}	2.26 (2)
Cd3—O16	2.356 (9)	Cd5—O25^{vii}	2.30 (2)
Cd3—O18	2.305 (18)		
Bond angles			
O2—Cd1—O1	53.3 (5)	O4—Cd4—O5^{iv}	142.9 (4)
O2—Cd1—O10^{i}	179.5 (5)	O4—Cd4—O6^{iv}	90.5 (9)
O7—Cd1—O1	141.3 (5)	O4—Cd4—O24	98.9 (7)
O7—Cd1—O2	88.1 (4)	O4—Cd4—O11^{v}	85.1 (4)
O7—Cd1—O19	91.6 (9)	O4—Cd4—O12^{v}	139.5 (4)
O7—Cd1—O10^{i}	91.5 (5)	O4—Cd4—O17^{vi}	84.7 (6)
O7—Cd1—O14^{ii}	89.2 (5)	O24—Cd4—O5^{iv}	92.6 (7)
O19—Cd1—O1	92.1 (7)	O24—Cd4—C17^{v}	83.6 (5)
O19—Cd1—O2	92.7 (7)	O6^{iv}—Cd4—O24	95.3 (11)
O19—Cd1—O10^{i}	87.1 (6)	O6^{iv}—Cd4—O5^{iv}	53.2 (9)
O10^{i}—Cd1—O1	127.2 (5)	O6^{iv}—Cd4—O12^{v}	130.0 (9)
O14^{ii}—Cd1—O1	87.3 (5)	O6^{iv}—Cd4—O17^{vi}	98.3 (9)
O14^{ii}—Cd1—O2	87.4 (4)	O11^{v}—Cd4—O24	86.0 (6)
O14^{ii}—Cd1—O19	179.2 (9)	O11^{v}—Cd4—O5^{iv}	131.1 (4)

O14^{ii}—Cd1—O10^{i}	92.8 (3)	O11^{v}—Cd4—O6^{iv}	175.6 (9)
O8—Cd2—O13	95.7 (4)	O11^{v}—Cd4—O12^{v}	54.4 (4)
O8—Cd2—O15	92.3 (3)	O11^{v}—Cd4—O17^{vi}	80.7 (4)
O8—Cd2—O20	170.8 (6)	O12^{v}—Cd4—O24	78.7 (5)
O8—Cd2—O13^{ii}	91.9 (4)	O17^{vi}—Cd4—O5^{iv}	92.7 (5)
O13—Cd2—O15	69.0 (2)	O17^{vi}—Cd4—O24	165.9 (5)
O20—Cd2—O13	93.1 (5)	O6—Cd5—O22	92.6 (13)
O20—Cd2—O15	88.3 (5)	O6—Cd5—O25	171.9 (12)
O10^{i}—Cd2—O8	81.9 (6)	O6—Cd5—O25^{vii}	104.2 (9)
O10^{i}—Cd2—O13	176.5 (4)	O21—Cd5—O3^{i}	89.1 (9)
O10^{i}—Cd2—O15	113.7 (3)	O21—Cd5—O6	108.9 (9)
O10^{i}—Cd2—O20	89.4 (6)	O21—Cd5—O22	84.0 (14)
O10^{i}—Cd2—O13^{ii}	101.3 (3)	O21—Cd5—O25^{vii}	146.5 (8)
O13^{ii}—Cd2—O13	76.10 (19)	O21—Cd5—O25	69.1 (8)
O13^{ii}—Cd2—O15	145.1 (2)	O25—Cd5—O22	94.9 (11)
O13^{ii}—Cd2—O20	92.8 (4)	O3^{i}—Cd5—O6	79.5 (12)
O16—Cd3—O6	172.5 (7)	O3^{i}—Cd5—O22	167.3 (11)
O18—Cd3—O6	107.0 (6)	O3^{i}—Cd5—O25	92.5 (9)
O18—Cd3—O16	70.8 (3)	O3^{i}—Cd5—O25^{vii}	92.1 (9)
O16^{iii}—Cd3—O6	109.8 (6)	O25^{vii}—Cd5—O22	99.5 (13)
O16^{iii}—Cd3—O16	72.5 (2)	O25^{vii}—Cd5—O25	77.4 (8)
O16^{iii}—Cd3—O18	143.2 (3)		

Symmetry codes: (i) *x*, -*y*-3/2, *z*-1/2; (ii) -*x*, -*y*-2, -*z*+1; (iii) -*x*+1, -*y*-2, -*z*+1; (iv) *x*, -*y*-3/2, *z*+1/2; (v) *x*+1, -*y*-3/2, *z*+1/2; (vi) -*x*+1, *y*+1/2, -*z*+3/2; (vii) -*x*+1, -*y*-1, -*z*+1; (viii) *x*-1, -*y*-3/2, *z*-1/2; (ix) -*x*+1, *y*-1/2, -*z*+3/2.

Table S7 The selected bond lengths and bond angles of **3**.

Empirical formula	$MnC_{15}H_{20}N_2O_7$
Formula weight	395.27
Temperature / K	293
Radiation / Å	0.71073 (Mo $K\alpha$)
Crystal system	Monoclinic
Space group	$P2_1/n$
a / Å	9.4648 (3)
b / Å	16.2782 (6)
c / Å	11.5458 (4)
α / °	90
β / °	97.104 (2)
γ / °	90
V / Å^3	1765.20 (11)
Z	4
F(000)	820
D_c./ g cm^{-3}	1.487
μ / mm^{-1}	0.79
Reflns coll.	18836
Unique reflns.	4396
R_{int}	0.043
$^aR_1$ [I$\geqslant$2σ(I)]	0.077
$^bwR_2$ (all data)	0.245
GOF	1.10
Void	55.3%
CCDC number	1943112

$^aR_1 = \sum||F_o| - |F_c||/\sum|F_o|$. $^bwR_2 = [\sum w(F_o^2 - F_c^2)^2/\sum w(F_o^2)^2]^{1/2}$.

Table S8 The selected bond lengths and bond angles of **3**.

Bond lengths			
Mn1—O1	1.927 (4)	Mn1—O4^{ii}	1.962 (4)
Mn1—O3^{i}	1.971 (4)	Mn1—O5^{iii}	1.930 (4)
Bond angles			
O1—Mn1—O3^{i}	99.38 (19)	O4^{ii}—Mn1—O3^{i}	114.29 (19)
O1—Mn1—O4^{ii}	113.5 (2)	O5^{iii}—Mn1—O3^{i}	110.09 (18)
O1—Mn1—O5^{iii}	125.77 (18)	O5^{iii}—Mn1—O4^{ii}	94.65 (17)

Symmetry codes: (i) *x*-1/2, -*y*+1/2, *z*-1/2; (ii) -*x*+3/2, *y*+1/2, -*z*+1/2; (iii) *x*+1/2, -*y*+1/2, *z*-1/2; (iv) *x*+1/2, -*y*+1/2, *z*+1/2; (v) -*x*+3/2, *y*-1/2, -*z*+1/2; (vi) *x*-1/2, -*y*+1/2, *z*+1/2.

Table S9 The selected bond lengths and bond angles of **4**.

Empirical formula	$Mn_3C_{47.5}N_3H_{75}O_{26.5}$
Formula weight	1276.92
Temperature / K	293
Radiation / Å	1.54184 Å (Cu *K*α)
Crystal system	Monoclinic
Space group	*C*2/*c*
a / Å	34.2808 (8)
b / Å	19.8399 (4)
c / Å	18.1612 (4)
α / °	90°
β / °	102.818 (2)
γ / °	90°
V / Å^3	12044.1 (5)
Z	8
F(000)	3648
D_c./ g cm^{-3}	0.996
μ / mm^{-1}	5.50
Reflns. coll.	34638
Unique reflns.	12181
R_{int}	0.044
$^aR_1$ [I≥2σ(I)]	0.098
$^bwR_2$ (all data)	0.301
GOF	1.06
Void	59.7%
CCDC number	1943142

$^aR_1 = \sum||F_o| - |F_c||/\sum|F_o|$. $^bwR_2 = [\sum w(F_o^2 - F_c^2)^2/\sum w(F_o^2)^2]^{1/2}$.

Table S10 The selected bond lengths and bond angles of **4**.

Bond lengths			
Mn1—O2	2.141 (4)	Mn2—O11^{ii}	2.262 (4)
Mn1—O8	2.163 (4)	Mn2—O12^{ii}	2.251 (4)
Mn1—O14	2.160 (4)	Mn3—O18	2.161 (4)
Mn1—O19	2.083 (4)	Mn3—O3^{i}	2.191 (4)
Mn1—O9^{i}	2.217 (4)	Mn3—O4^{iii}	2.172 (4)
Mn2—O1	2.147 (4)	Mn3—O5^{iv}	2.198 (5)
Mn2—O7	2.138 (4)	Mn3—O6^{iv}	2.363 (5)
Mn2—O13	2.132 (4)	Mn3—O17^{v}	2.148 (4)
Mn2—O10^{i}	2.154 (4)		
Bond angles			
O2—Mn1—O8	85.84 (19)	O10^{i}—Mn2—O11^{ii}	142.08 (17)
O2—Mn1—O14	150.54 (17)	O10^{i}—Mn2—O12^{ii}	85.42 (17)
O2—Mn1—O9^{i}	94.16 (18)	O12^{ii}—Mn2—O11^{ii}	56.70 (16)
O14—Mn1—O8	89.3 (2)	O3^{i}—Mn3—O5^{iv}	95.5 (2)
O14—Mn1—O9^{i}	86.54 (18)	O3^{i}—Mn3—O6^{iv}	96.3 (2)
O19—Mn1—O2	104.6 (2)	O4^{iii}—Mn3—O3^{i}	92.1 (2)
O19—Mn1—O8	96.03 (19)	O4^{iii}—Mn3—O5^{iv}	82.55 (19)
O19—Mn1—O14	104.8 (2)	O4^{iii}—Mn3—O6^{iv}	137.42 (17)
O19—Mn1—O9^{i}	92.13 (17)	O5^{iv}—Mn3—O6^{iv}	55.18 (19)
O8—Mn1—O9^{i}	171.57 (17)	O17^{v}—Mn3—O3^{i}	163.76 (18)
O1—Mn2—O10^{i}	85.5 (2)	O17^{v}—Mn3—O4^{iii}	85.6 (2)
O1—Mn2—O11^{ii}	102.7 (2)	O17^{v}—Mn3—O5^{iv}	100.2 (2)
O1—Mn2—O12^{ii}	102.1 (2)	O17^{v}—Mn3—O6^{iv}	96.2 (2)
O7—Mn2—O1	83.3 (2)	O17^{v}—Mn3—O18	85.6 (2)
O7—Mn2—O10^{i}	127.12 (17)	O18—Mn3—O3^{i}	84.8 (2)
O7—Mn2—O11^{ii}	90.76 (16)	O18—Mn3—O4^{iii}	135.54 (17)
O7—Mn2—O12^{ii}	147.46 (16)	O18—Mn3—O5^{iv}	141.91 (19)
O13—Mn2—O1	153.9 (2)	O18—Mn3—O6^{iv}	86.87 (17)
O13—Mn2—O7	84.8 (2)	O13—Mn2—O11^{ii}	100.6 (2)
O13—Mn2—O10^{i}	83.3 (2)	O13—Mn2—O12^{ii}	100.5 (2)

Symmetry codes: (i) -*x*+3/2, *y*+1/2, -*z*+1/2; (ii) *x*, -*y*+1, *z*-1/2; (iii) *x*-1/2, *y*+1/2, *z*; (iv) -*x*+3/2, -*y*+3/2, -*z*+1; (v) -*x*+1, *y*, -*z*+1/2; (vi) -*x*+3/2, *y*-1/2, -*z*+1/2; (vii) *x*+1/2, *y*-1/2, *z*; (viii) *x*, -*y*+1, *z*+1/2.

Table S11 The selected bond lengths and bond angles of **5**.

Empirical formula	$Zn_5C_{60}H_{73}N_7O_{29}$
Formula weight	1683.30
Temperature / K	293
Radiation / Å	0.71073 (Mo *K*α)
Crystal system	Monoclinic
Space group	*C*2/*c*
a / Å	30.2857 (13)
b / Å	16.9980 (7)
c / Å	28.4898 (12)
α / °	90
β / °	95.403 (2)
γ / °	90
V / Å^3	14601.3 (11)
Z	8
F(000)	5520
D_c./ g cm^{-3}	1.252
μ / mm^{-1}	1.69
Reflns coll.	64906
Unique reflns.	14346
R_{int}	0.108
$^aR_1$ [I≥2σ(I)]	0.134
$^bwR_2$ (all data)	0.400
GOF	1.06
Void	41.6%
CCDC number	1943098

$^aR_1 = \sum||F_o| - |F_c||/\sum|F_o|$. $^bwR_2 = [\sum w(F_o^2 - F_c^2)^2/\sum w(F_o^2)^2]^{1/2}$.

Table S12 The selected bond lengths and bond angles of **5**.

Bond lengths			
Zn1—O1	1.943 (11)	Zn3—O6^{iv}	1.909 (18)
Zn1—O8	1.982 (10)	Zn4—O5	2.032 (11)
Zn1—O16^{i}	1.994 (11)	Zn4—O25	2.30 (2)
Zn1—O18^{ii}	2.009 (9)	Zn4—O14^{iv}	2.048 (10)
Zn1—C26^{i}	2.567 (13)	Zn4—O20^{iv}	2.035 (11)
Zn2—O2	1.888 (12)	Zn4—O11^{v}	2.187 (15)
Zn2—O7	1.944 (10)	Zn4—O12^{v}	2.193 (15)
Zn2—O17^{ii}	1.990 (9)	Zn5—O9	2.031 (12)
Zn2—O22^{iii}	1.930 (10)	Zn5—O26	1.969 (11)
Zn3—O3	1.933 (9)	Zn5—O10^{vi}	2.014 (12)
Zn3—O13	1.894 (12)	Zn5—O23^{vii}	2.026 (10)
Zn3—O19	1.909 (12)	Zn5—O24^{viii}	2.037 (10)
Bond angles			
O1—Zn1—O8	118.0 (6)	O5—Zn4—O11^{v}	92.8 (5)
O1—Zn1—O16^{i}	111.5 (6)	O5—Zn4—O12^{v}	151.4 (5)
O1—Zn1—O18^{ii}	110.2 (5)	O14^{iv}—Zn4—O25	173.7 (6)
O8—Zn1—O16^{i}	115.9 (5)	O14^{iv}—Zn4—O11^{v}	95.8 (6)
O8—Zn1—O18^{ii}	99.0 (4)	O14^{iv}—Zn4—O12^{v}	91.4 (5)
O16^{i}—Zn1—O18^{ii}	99.6 (4)	O20^{iv}—Zn4—O25	77.1 (7)
O2—Zn2—O7	O2—Zn2—O7	O20^{iv}—Zn4—O14^{iv}	102.0 (5)
119.6 (5)	119.6 (5)	O20^{iv}—Zn4—O11^{v}	142.1 (6)
O2—Zn2—O17^{ii}	O2—Zn2—O17^{ii}	O20^{iv}—Zn4—O12^{v}	87.0 (5)
115.4 (5)	115.4 (5)	O9—Zn5—O24^{viii}	86.3 (5)
O2—Zn2—O22^{iii}	O2—Zn2—O22^{iii}	O10^{vi}—Zn5—O9	158.2 (6)
103.8 (5)	103.8 (5)	O10^{vi}—Zn5—O23^{vii}	86.3 (5)
O13—Zn3—O3	115.7 (5)	O10^{vi}—Zn5—O24^{viii}	90.2 (5)
O13—Zn3—O19	119.5 (6)	O23^{vii}—Zn5—O9	88.9 (5)
O13—Zn3—O6^{iv}	105.0 (6)	O23^{vii}—Zn5—O24^{viii}	158.1 (4)
O19—Zn3—O3	107.6 (5)	O26—Zn5—O9	97.1 (6)
O5—Zn4—O25	77.8 (7)	O26—Zn5—O10^{vi}	104.7 (6)

O5—Zn4—O14^{iv}	97.4 (5)	O26—Zn5—O23^{vii}	106.2 (5)
O5—Zn4—O20^{iv}	117.3 (5)	O26—Zn5—O24^{viii}	95.6 (5)

Symmetry codes: (i) -*x*+1, *y*, -*z*+3/2; (ii) *x*-1/2, *y*+1/2, z; (iii) *x*, *y*+1, *z*; (iv) -*x*+1, -*y*+1, -*z*+1; (v) *x*, -*y*+2, *z*-1/2; (vi) -*x*+1/2, -*y*+3/2, -*z*+2; (vii) -*x*+1/2, *y*+1/2, -*z*+3/2; (viii) *x*, -*y*+1, *z*+1/2; (ix) *x*, -*y*+2, *z*+1/2; (x) *x*+1/2, *y*-1/2, *z*; (xi) *x*, *y*-1, *z*; (xii) -*x*+1/2, *y*-1/2, -*z*+3/2; (xiii) *x*, -*y*+1, *z*-1/2

.

Table S13 The calculated coordination geometry of each metal centre in compounds **1~5** by Shape 4.0, based on the smaller Continuous Shape Measures (CShM) value.

Compounds	Metal ions	Coordination Numbers	Geometry	CShM Value
1	Cd1	7	Capped trigonal prism (CTPR-7)	2.235
2	Cd1	7	Pentagonal bipyramid (PBPY-7)	2.532
	Cd2	6	Octahedron (OC-6)	2.845
	Cd3	4	Square (SP-4)	3.761
	Cd4	7	Pentagonal bipyramid (PBPY-7)	2.108
	Cd5	6	Octahedron (OC-6)	2.945
3	Mn1	4	Tetrahedron (T-4)	1.441
4	Mn1	6	Octahedron (OC-6)	5.632
	Mn2	6	Trigonal prism (TPR-6)	7.235
	Mn3	6	Trigonal prism (TPR-6)	6.911
5	Zn1	4	Tetrahedron (T-4)	0.598
	Zn2	4	Tetrahedron (T-4)	1.904
	Zn3	4	Tetrahedron (T-4)	0.513
	Zn4	6	Octahedron (OC-6)	4.181
	Zn5	5	Spherical square pyramid (SPY-5)	0.320

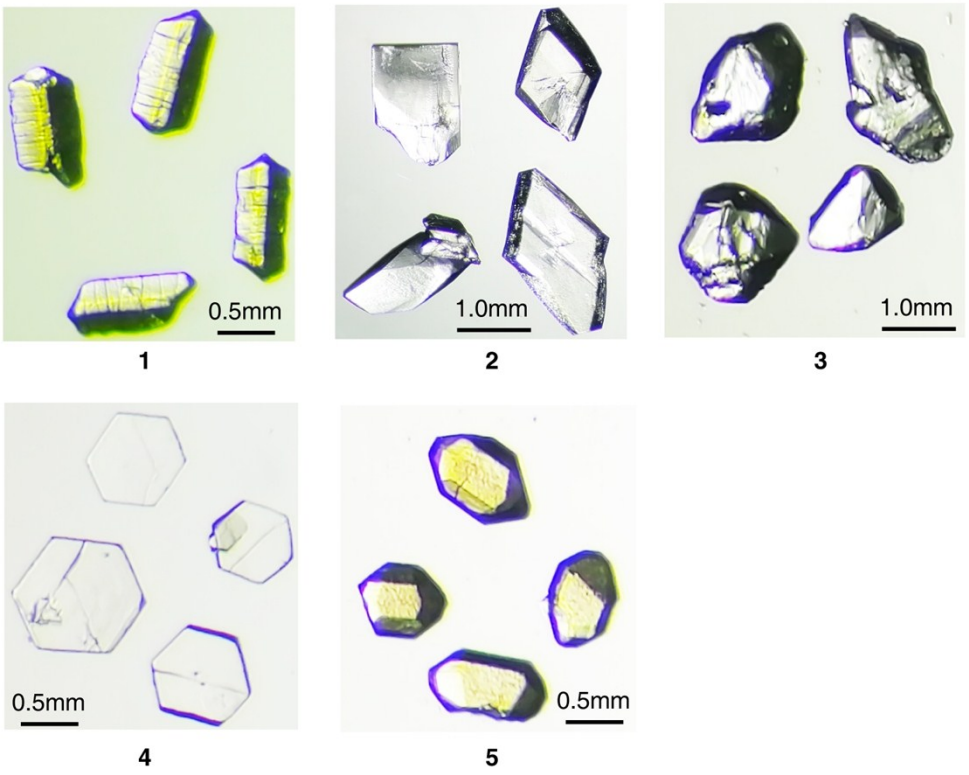

Figure S1 The photos of the as-synthesized crystals of the MOFs of **1**~**5** in this work.

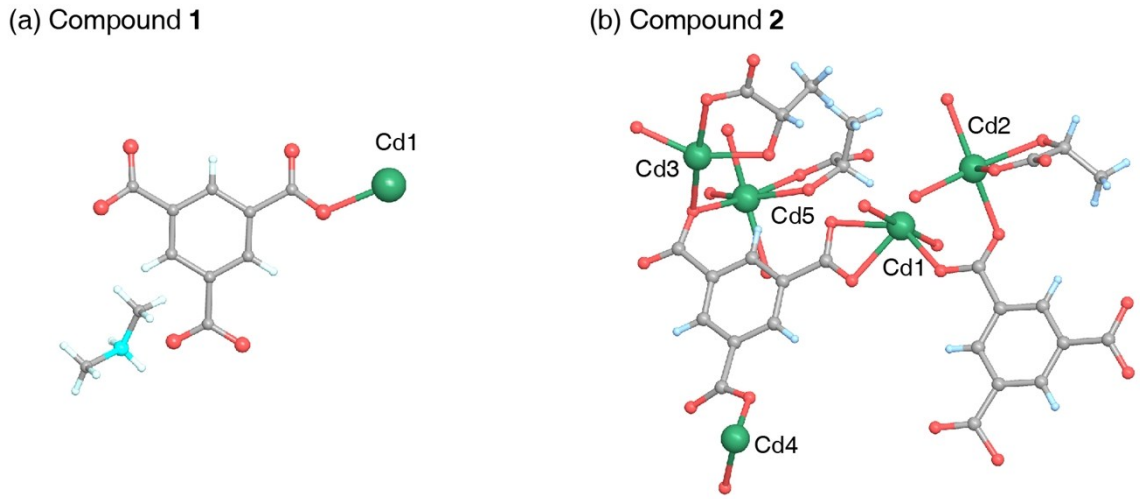

Figure S2 View of crystallographic asymmetric unit of (a) **1** and (b) **2**.

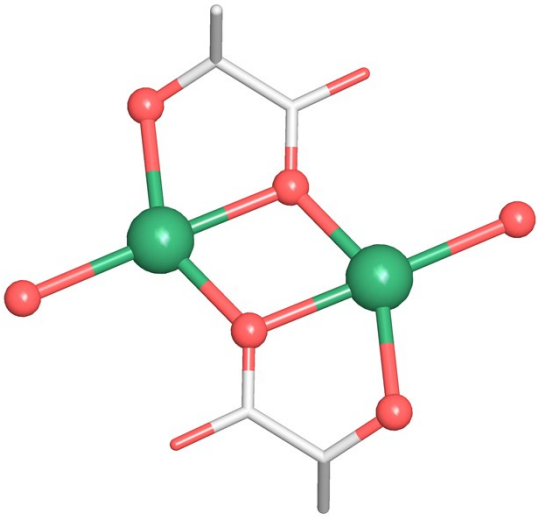

Figure S3 Structure view of the planar tetragonal coordination geometry of Cd3 in compound **2**.

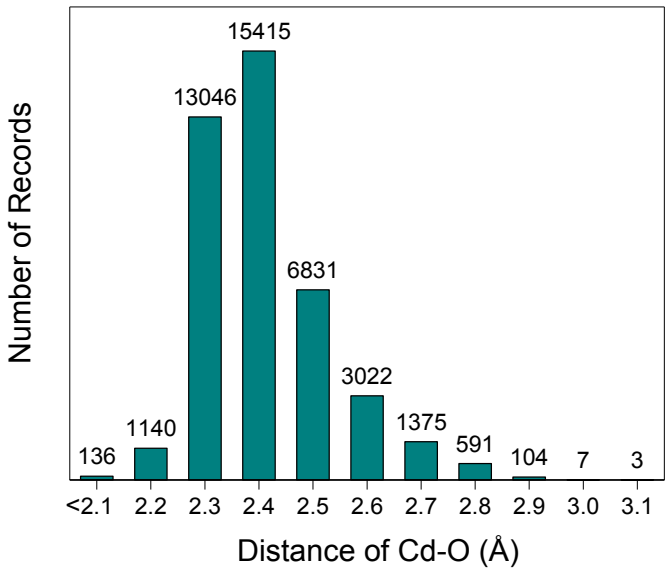

Figure S4 The statistics in histogram showing the distribution of Cd-O bond lengths in the CSD database (Version 2019).

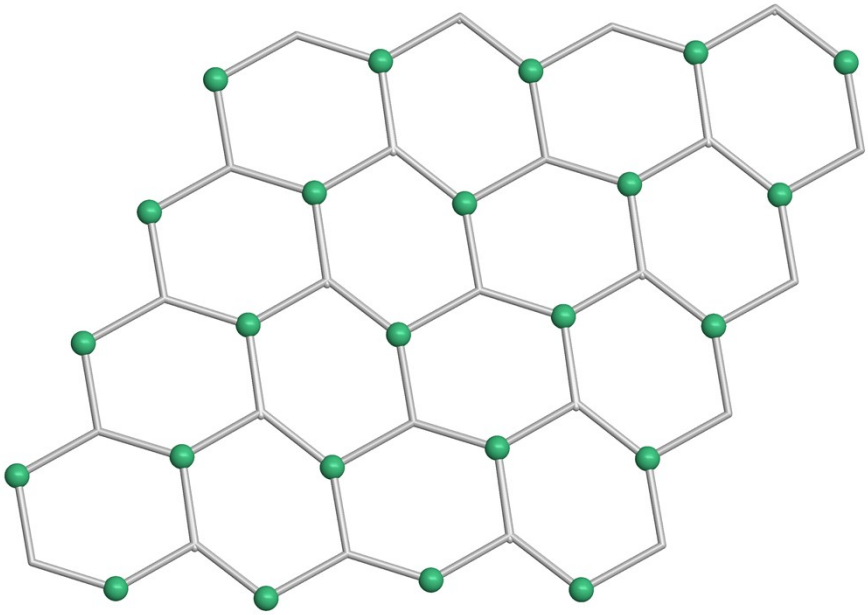

Figure S5 Structure view of the (3,6)-connected layer of compound **2**.

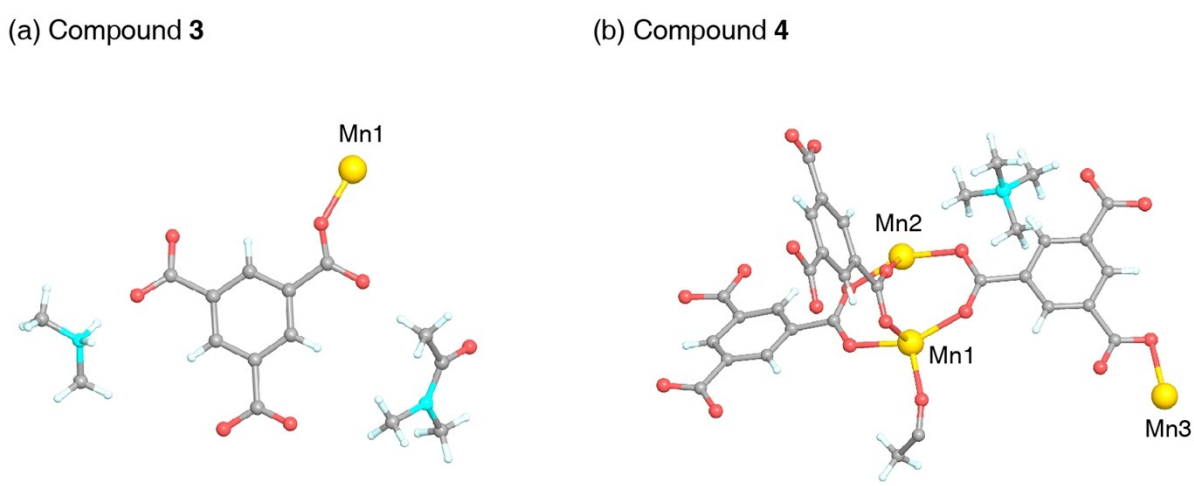

Figure S6 View of crystallographic asymmetric unit of (a) **3** and (b) **4**.

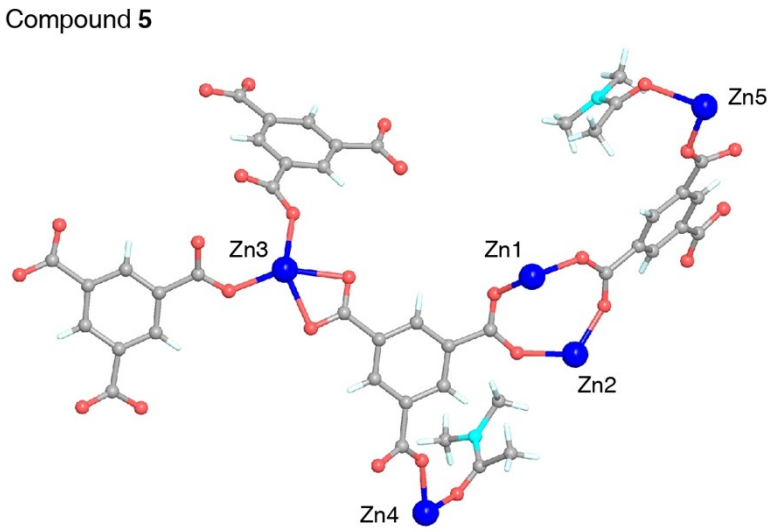

Figure S7 View of crystallographic asymmetric unit of **5**.

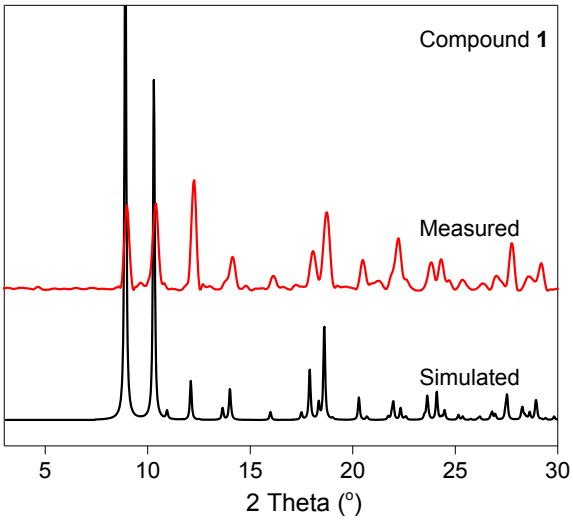

Figure S8 The simulated (black) and measured (red) PXRD patterns of **1**. The measured results were consistent with the simulated diffraction peaks, excepting the difference in intensity of each peak due to anisotropy of the crystals.

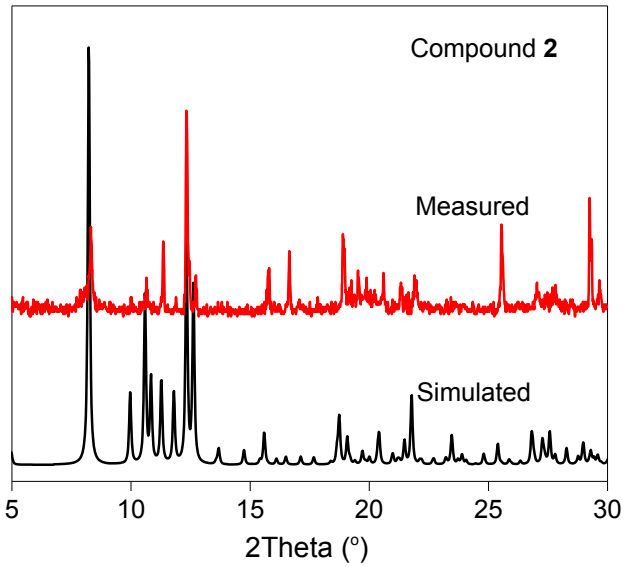

Figure S9 The simulated (black) and measured (red) PXRD patterns of **2**.

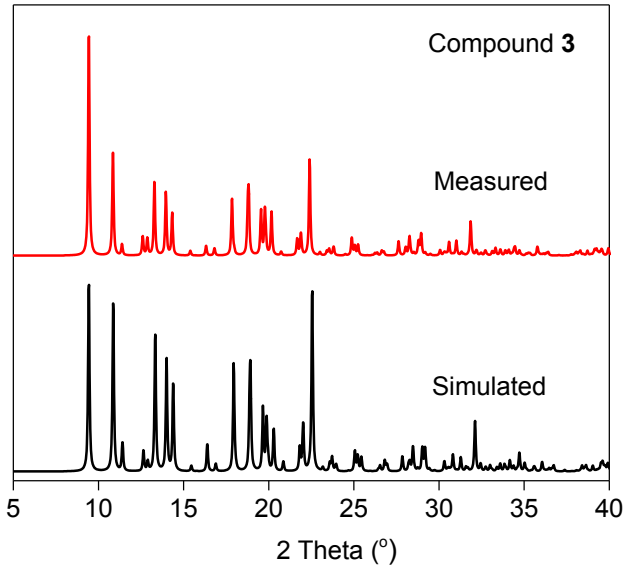

Figure S10 The simulated (black) and measured (red) PXRD patterns of **3**.

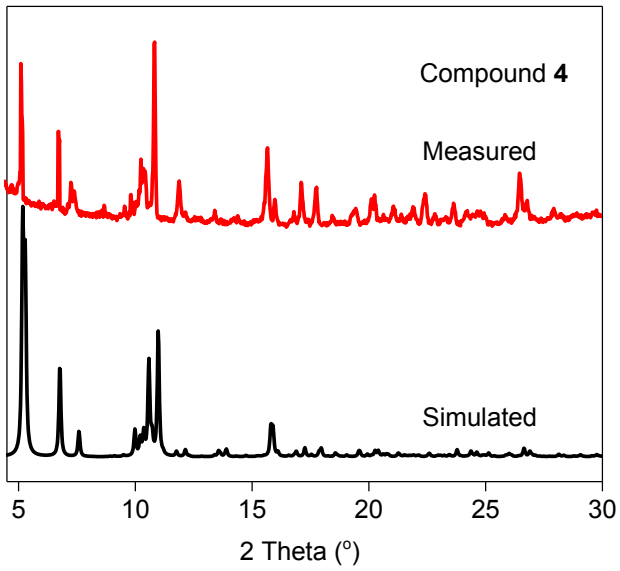

Figure S11 The simulated (black) and measured (red) PXRD patterns of **4**.

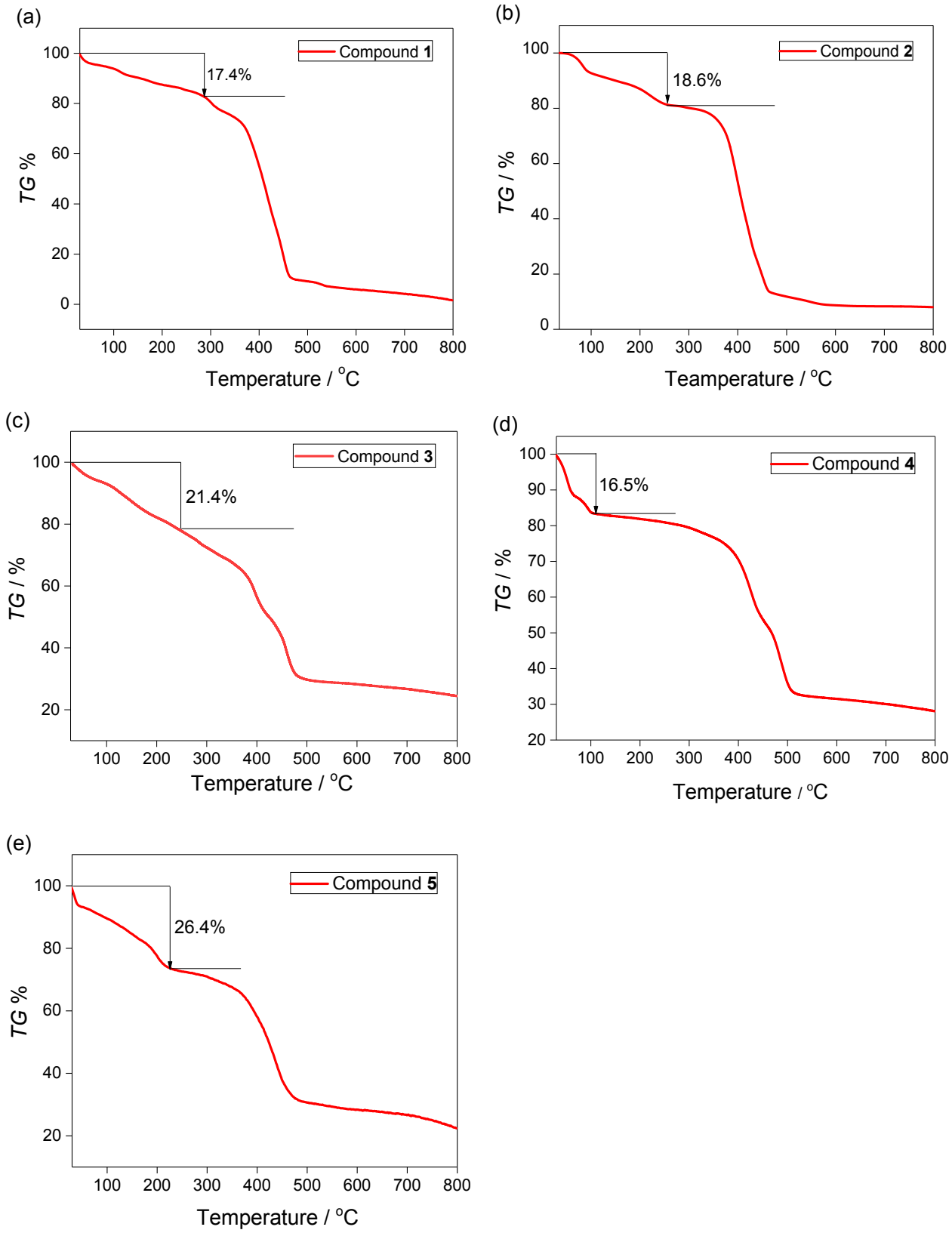

Figure S12 The thermogravimetric curves of MOFs of **1**~**5**. For **1**, the first weight loss of 17.4% till 300 °C was corresponding to the departure of 0.5 DMA and 2 H_2O per formula (Cal. 17.8%). For **2**, the first weight loss of 18.6% till 250 °C was corresponding to the departure of 4 DMF per formula

(Cal. 17.8%). For **3**, The compound exhibited continuous weight loss without evident platform. There was a weigh loss of 21.4% before the spinodal at 250 °C, which is attributed to the departure of guest DMA (Cal. 22.0%). Under further heating, continuous weight loss was observed, indicating the decomposition of the negative framework. For **4**, the first weight loss of 16.5% till 110 °C was corresponding to the departure of 6.5 CH_3OH per formula (Cal. 16.2%). For **5**, the first weight loss of 26.4% till 230 °C was corresponding to the departure of 3 guest and 2 coordinated DMA per formula (Cal. 25.8%).

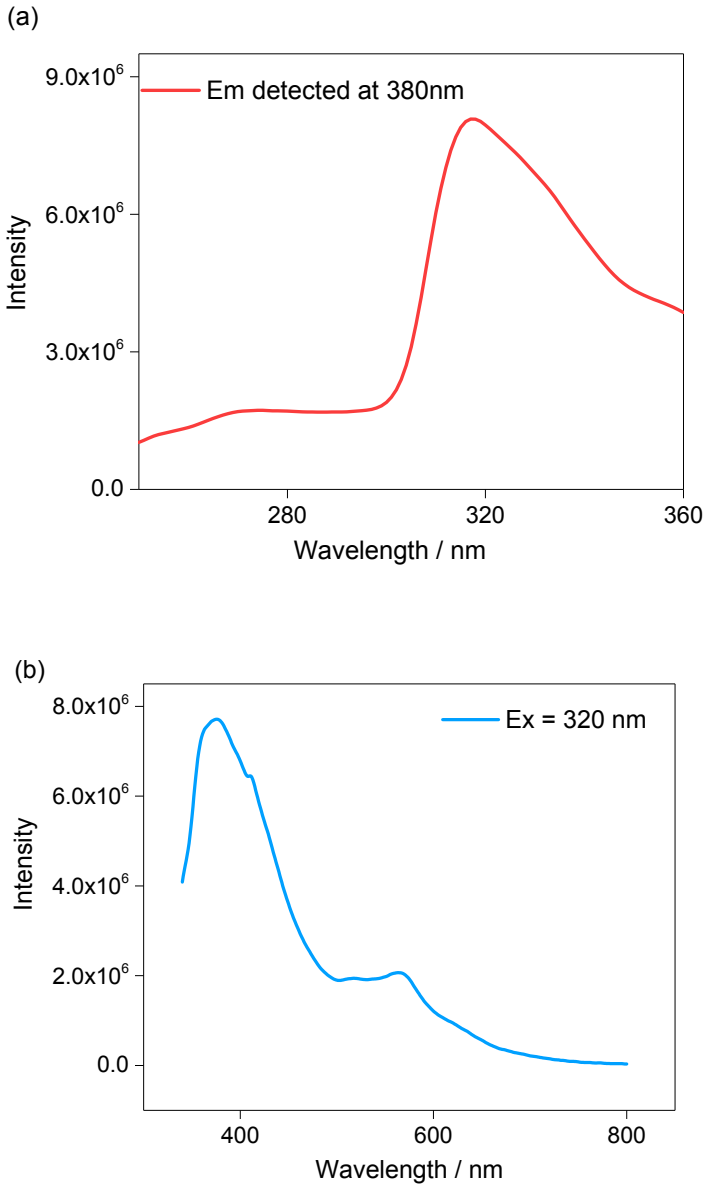

Figure S13 The (a) emission and (b) excitation spectra of the free ligand H_3btc.

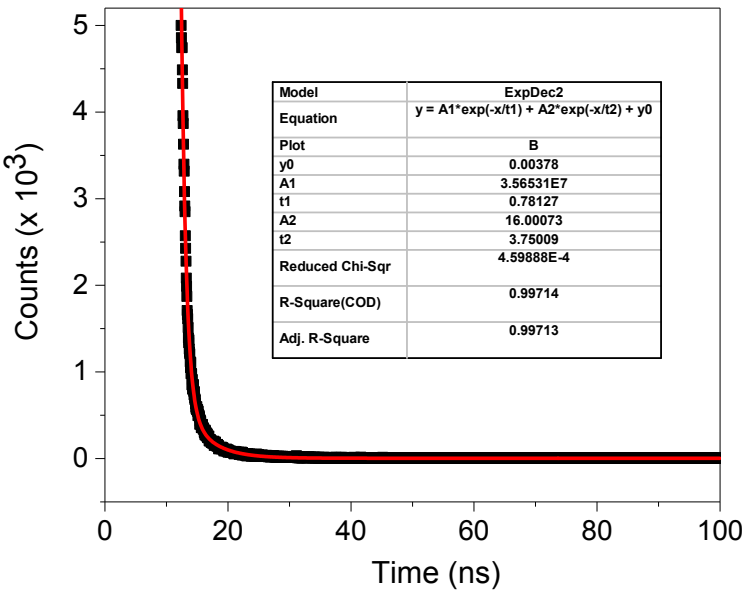

Figure S14 The decay time dependent emission intensity (black square) of the free ligand of H_3btc under excitation of 320 nm and detected emission at 380 nm, giving the fitted (red line) fluorescence lifetime of 0.78 ns for H_3btc.

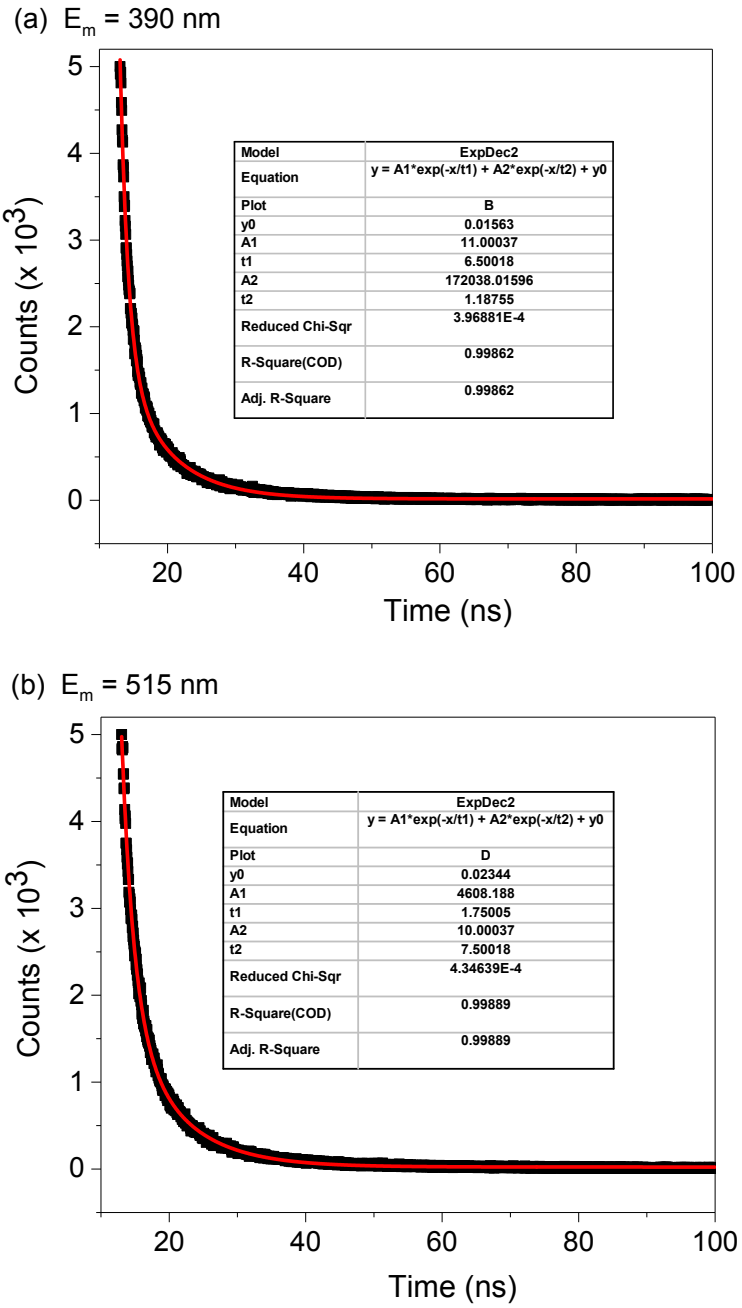

Figure S15 The decay time dependent emission intensity (black square) of **1** under excitation of 330 nm, giving the fitted (red line) fluorescence lifetime of 6.5 ns for the emission at 390 nm (a), and 1.7 ns for the emission at 515 nm (b).

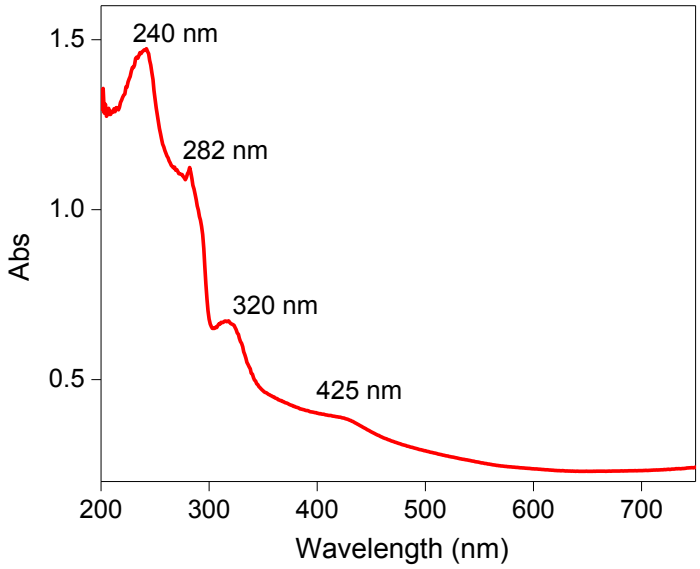

Figure S16 The solid-state UV diffuse reflectance spectrum of **1**.

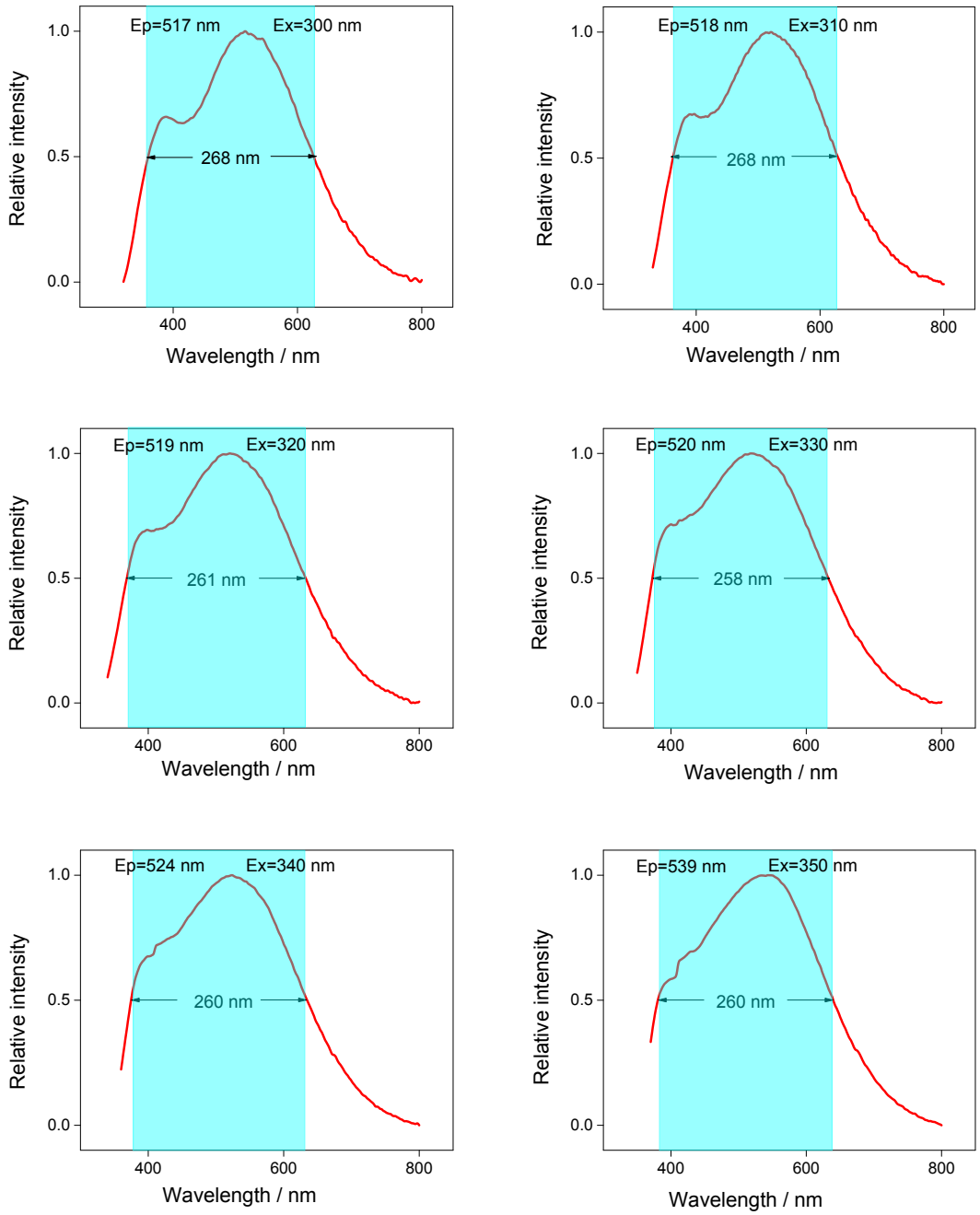

Figure S17 The solid-state fluorescence emission spectra with the peak position (E_p) of **1** under different excitation (E_x). The region of full width at half maxima of each spectrum was highlighted in cyan.

Table S14 Statistics of the full width at half maxima (FWHM) for the solid-state emission spectra of **1** under different excitation of 300~350 nm.

E_x/nm	E_p[a]/nm	E_{m1}[b]/nm	E_{m2}[c]/nm	FWHM / nm	CIE (*x*, *y*)	Color Temperature	CRI
300	517	358	626	268	(0.303, 0.363)	5899	90
310	518	361	629	268	(0.305, 0.360)	5882	90
320	519	370	631	261	(0.306, 0.358)	5874	90
330	520	373	631	258	(0.305, 0.354)	5891	90
340	524	374	634	260	(0.307, 0.356)	5886	90
350	539	380	640	260	(0.317, 0.364)	5773	89

[a] Location of the emission spectrum with the maximum intensity. [b] The start point of emission spectrum with half maxima intensity. [c] The end point of emission spectrum with half maxima intensity.

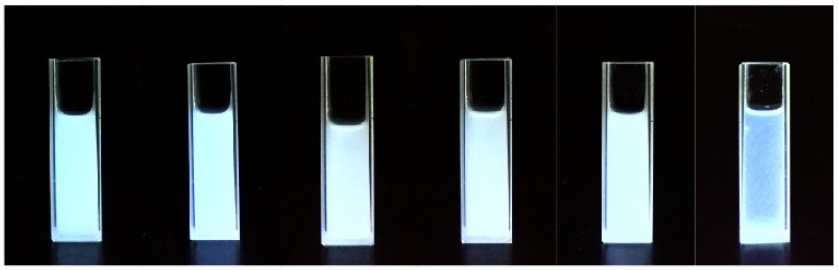

Figure S18 Photos of the fluorescence emission of suspension of **1** in different organic solvents, under excitation of 365 nm using an ultraviolet lamp. The suspensions were prepared by dispersing 5 mg fine-ground crystals of **1** into 3 mL solvent, followed by ultrasonic treatment for 10 minutes.

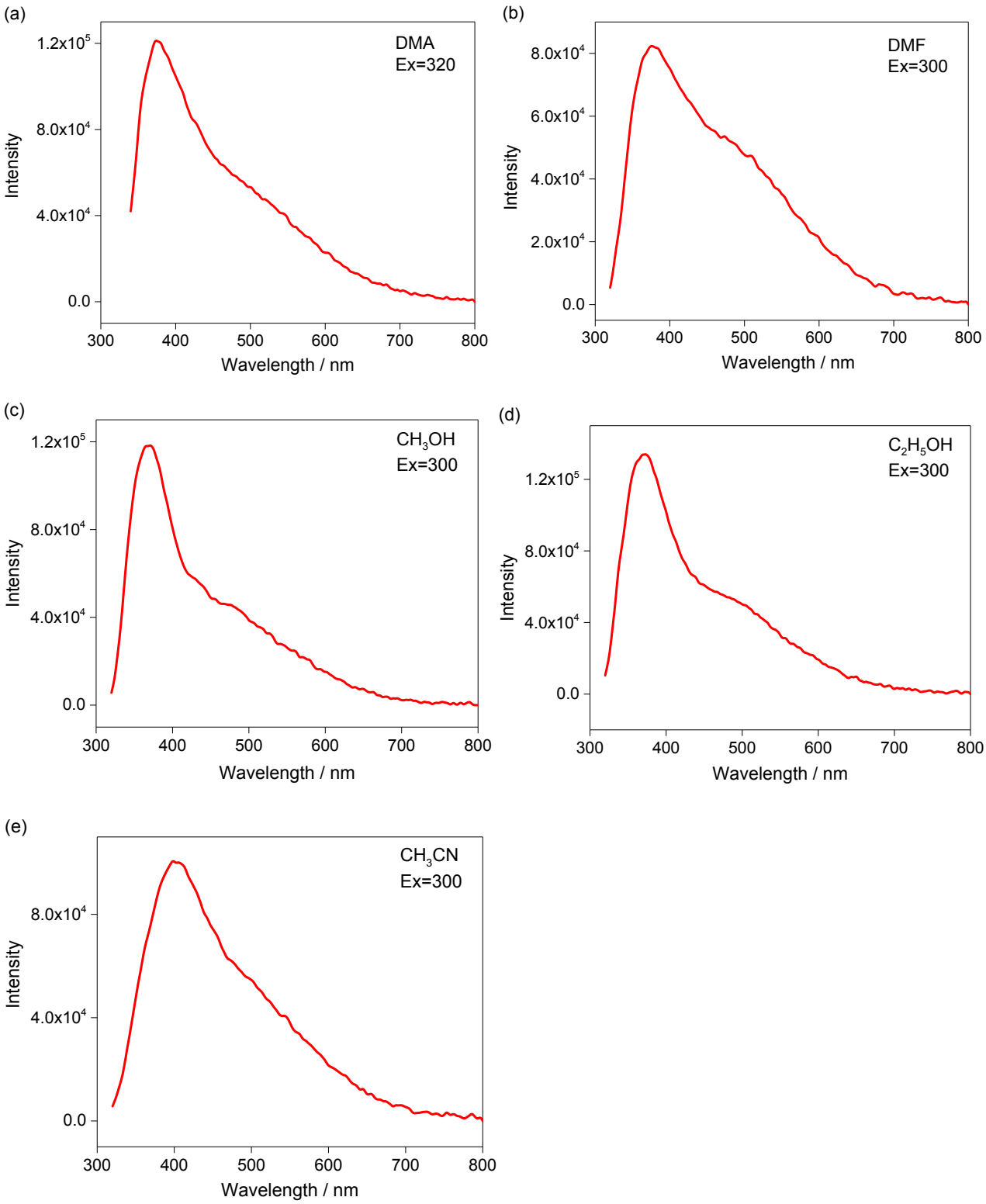

Figure S19 The solution-state emission spectra of **1** in various solvents of DMA, DMF, CH_3OH, C_2H_5OH, CH_3CN and CH_2Cl_2, under different excitation, which also exhibited continuous and broadband spectra.

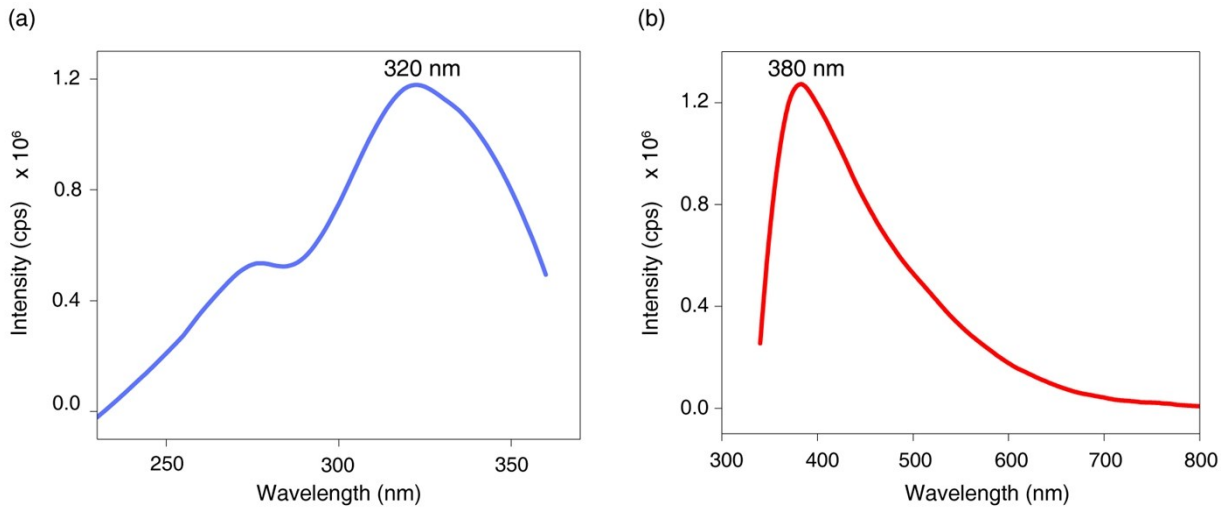

Figure S20 (a) The solid-state fluorescence excitation spectrum of **2** detected at an emission of 380 nm. (b) The solid-state fluorescence emission spectrum of **2** excited at a radiation of 320 nm.

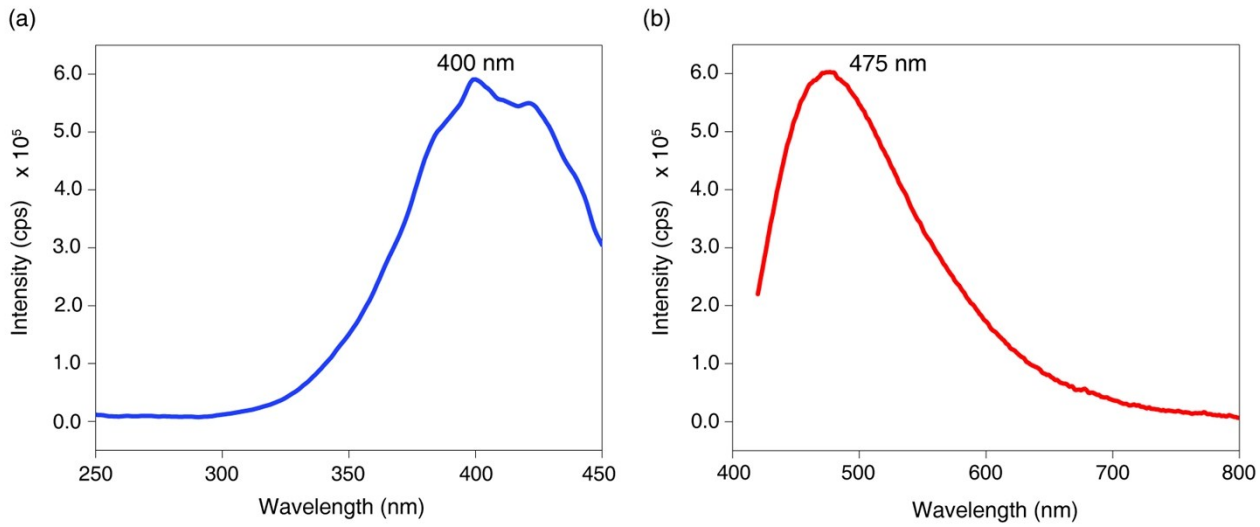

Figure S21 (a) The solid-state fluorescence excitation spectrum of **3** detected at an emission of 475 nm. (b) The solid-state fluorescence emission spectrum of **3** excited at a radiation of 400 nm.

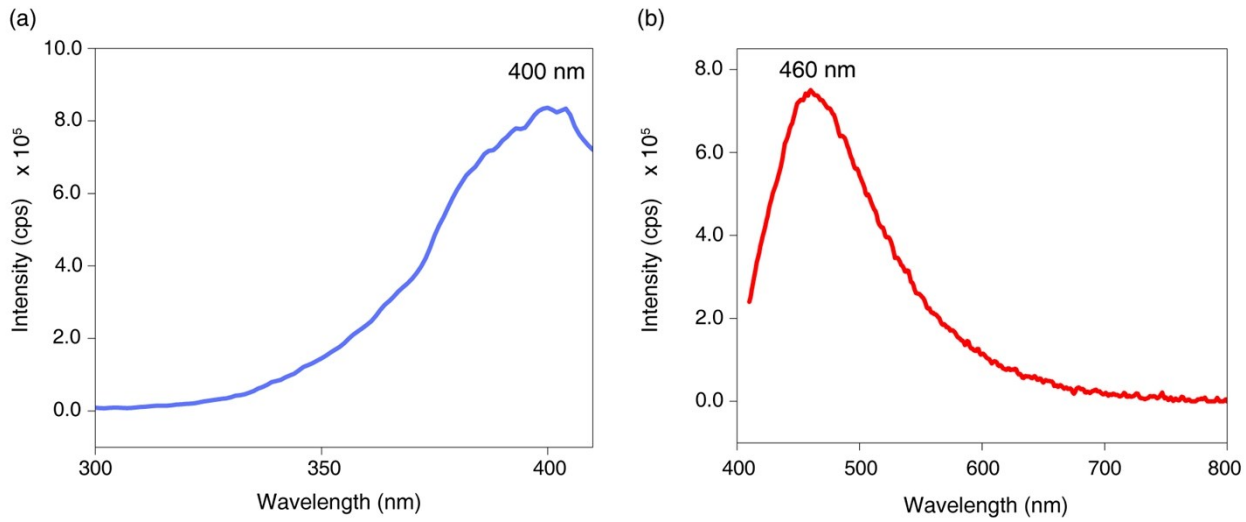

Figure S22 (a) The solid-state fluorescence excitation spectrum of **4** detected at an emission of 460 nm. (b) The solid-state fluorescence emission spectrum of **4** excited at a radiation of 400 nm.

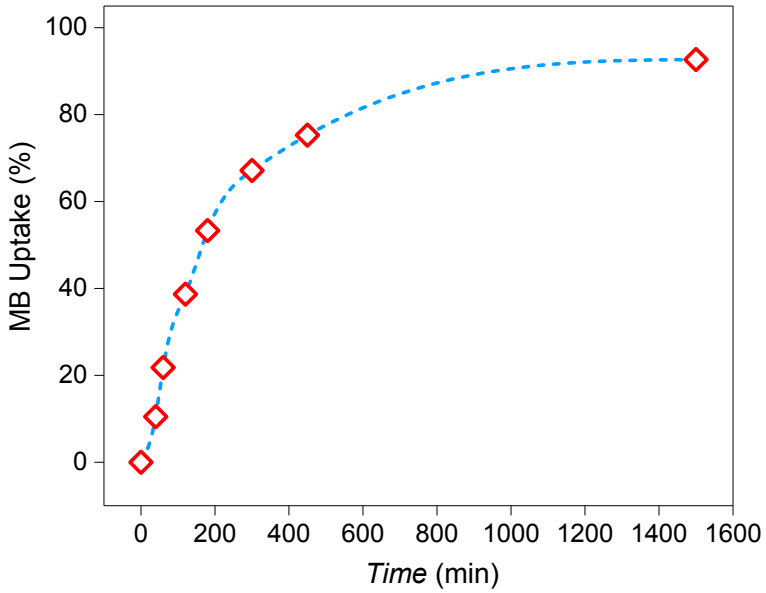

Figure S23 The time dependent MB uptake of **1**, with an initial MB concentration of 20 mg L^{-1}.

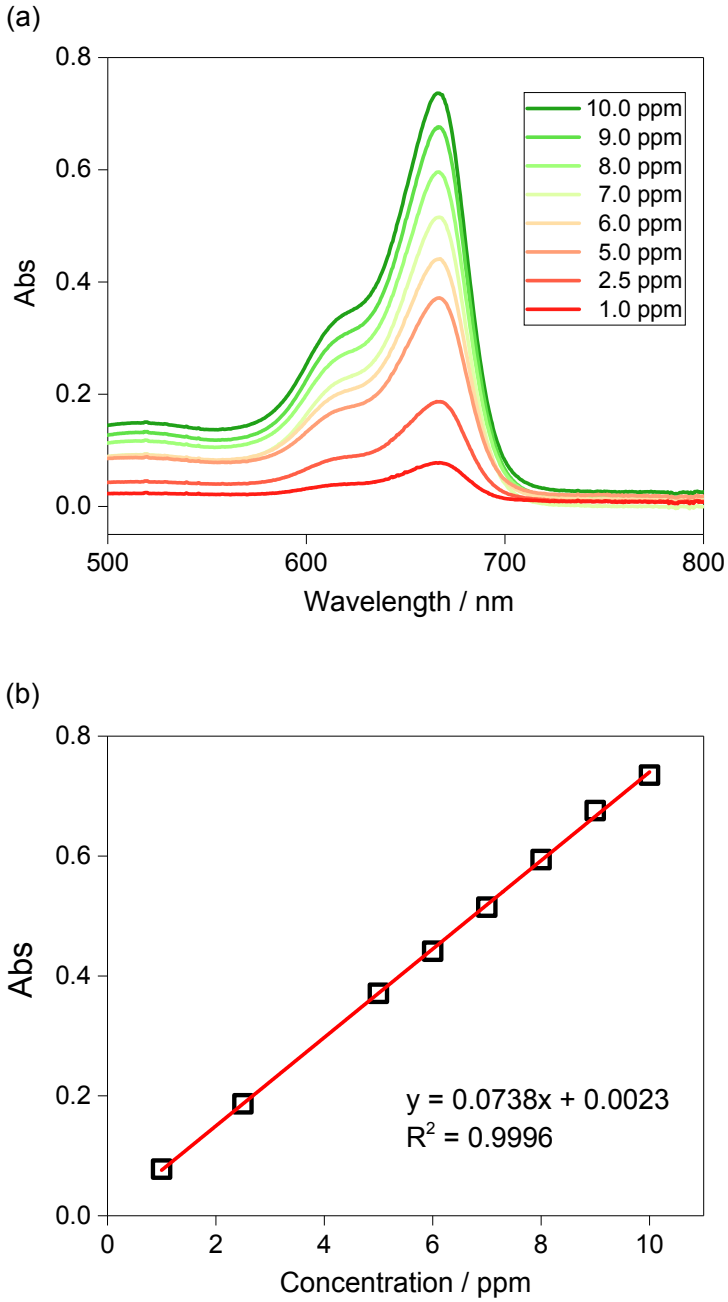

Figure S24 (a) The standard concentration dependent UV-vis spectra of MB. (b) The linear relationship between the absorbance and concentration of MB.

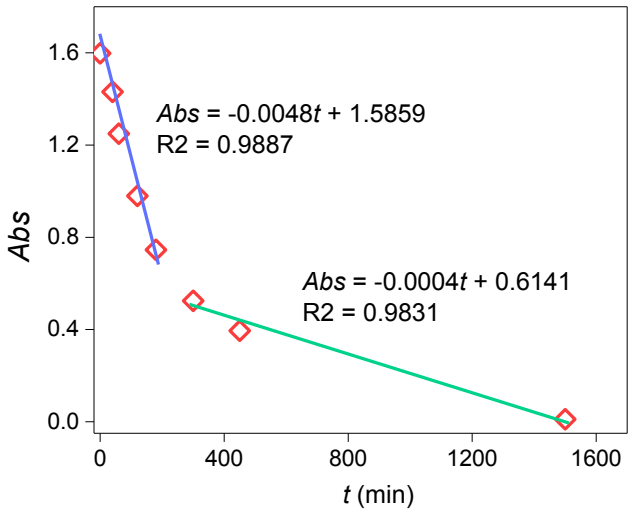

Figure S25 The time dependent absorbance evolution of MB, showing two different first-order adsorption mechanism.

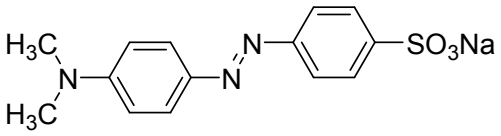

Figure S26 The structure view of anionic dye of methyl yellow (MO).

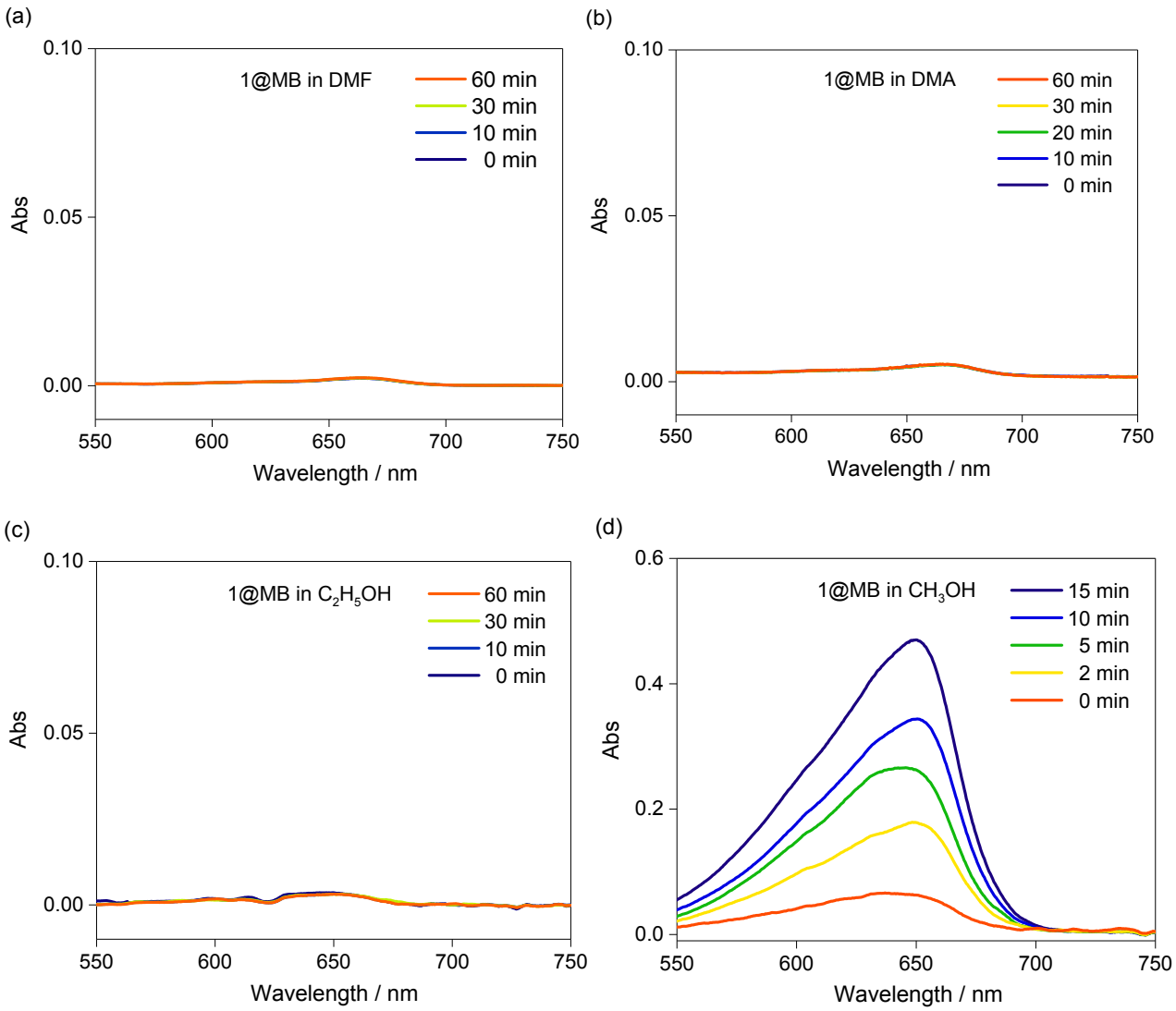

Figure S27 The MB releasing behaviors of the dye captured crystals of **1** in different organic solutions of (a) DMF, (b) DMA, (c) C_2H_5OH, and (d) CH_3OH.

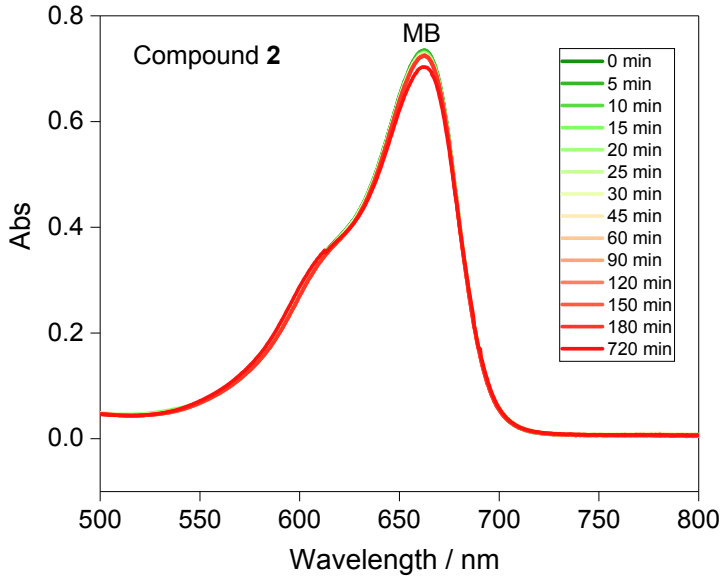

Figure S28 The time dependent sorption behaviors of **2** toward MB in DMF solution with a concentration of 10 mg L^{-1}.

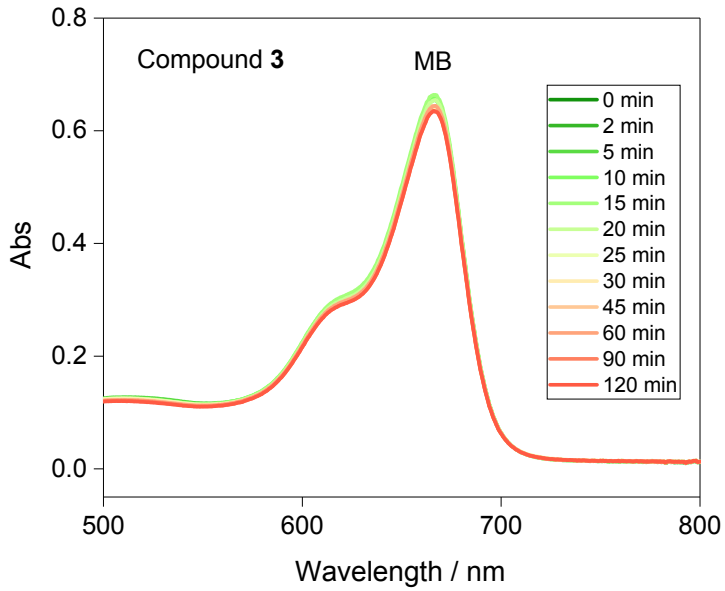

Figure S29 The time dependent sorption behaviors of **3** toward MB in DMF solution with a concentration of 10 mg L^{-1}.

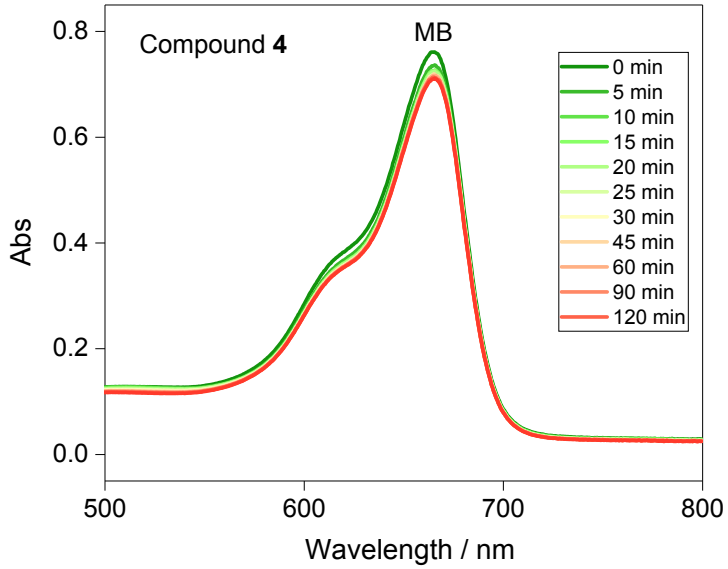

Figure S30 The time dependent sorption behaviors of **4** toward MB in DMF solution with a concentration of 10 mg L^{-1}.